Resonant production of color octet muons at Future Circular Collider-based muon-proton colliders *

Y. C. Acar[1;1)] U. Kaya[1,2;2)] B. B. Oner[1;3)]

[1] Department of Material Science and Nanotechnology, TOBB University of Economics and Technology, Ankara 06560, Turkey
[2] Department of Physics, Ankara University, Ankara 06560, Turkey

Abstract: We investigate the resonant production of color octet muons in order to explore the discovery potential of Future Circular Collider (FCC)-based μp colliders. It is shown that the search potentials of μp colliders essentially surpass the potential of the LHC and would exceed that of the FCC pp collider.

Keywords: leptogluons, lepton-hadron interactions, composite models, muon-proton colliders, color octet muon, beyond the standard model

PACS: 13.60.-r, 12.60.Rc **DOI:** 10.1088/1674-1137/42/8/083108

1 Introduction

High energy physics experiments performed in recent decades show that the Standard Model (SM) is consistent in the low energy regime. However, there are still phenomenological and theoretical problems and questions to be answered. Experimental research on new physics, searching for these answers for higher energies, relies on recently developed accelerator technologies. Energy frontier lepton colliders seem to be prominent candidates to investigate the validity of the SM at high energies, and they have the potential to reveal novelties that lie beyond the Standard Model (BSM). Producing and colliding muon beams with intense bunches to achieve sufficiently high luminosities is still a promising topic. In this regard, a recent paper by the Muon Accelerator Program (MAP) addressed designs for various center-of-mass (CM) energy muon colliders (μC) from 126 GeV (Higgs factory) to multi-TeV (energy frontier) options [1]. Also, ultimate case muon colliders with CM energy up to 100 TeV were considered in another study, and parameters of these colliders were given [2].

Developing the technology of lepton colliders makes high luminosity and high CM energy lepton-hadron colliders possible. In this manner, one can utilize the advantages of their vital role in understanding the fundamental structure of matter using the highest energy hadron beams, which will be provided by the Future Circular Collider (FCC) [3]. In the near future, it is expected that the construction of μp machines can also be considered, depending on the solutions to the principal issues of the $\mu^+\mu^-$ colliders. Some advantages of the highest energy μp machines can be listed briefly as follows. Firstly, multi-TeV scale muon-proton collisions would test the mechanisms of composite models and may give us clear hints about the fermion mixing and generation replication puzzle of the SM fermions. In addition, they would present experimental results that enable us to understand QCD better. Exotic particle production is more probable compared to ep colliders, because of the large mass ratio between muon and electron [4].

Muon-proton colliders were first proposed two decades ago. Construction of an additional proton ring in a $\sqrt{s}$= 4 TeV muon collider tunnel was suggested in Ref. [4] to handle a μp collider with the same CM energy. However, the luminosity value, $L_{\mu p}=3\times10^{35}$ cm^{-2}s^{-1}, was greatly overestimated. A realistic value for this should be three orders of magnitude smaller [5]. Then, construction of an additional 200 GeV energy muon ring in the Tevatron tunnel in order to handle a $\sqrt{s}$ = 0.9 TeV μp collider with $L_{\mu p}$=10^{32} cm^{-2}s^{-1} was considered in Ref. [6]. In Ref. [5], the ultimate case of muon beams with 50 TeV energy [2] was considered as an option for 100 TeV CM energy μp colliders, assuming that a 50 TeV proton ring would be added into the μC tunnel, and a luminosity value $\sim 10^{33}$ cm^{-2}s^{-1} was estimated. The

Received 17 July 2017, Revised 11 May 2018, Published online 9 July 2018
∗ Supported by TUBITAK (114F337)
1) E-mail: ycacar@etu.edu.tr
2) E-mail: ukaya@etu.edu.tr
3) E-mail: b.oner@etu.edu.tr

main parameter calculations of FCC-based muon-proton and muon-lead ion colliders were given in a recent paper which considers beam-beam effects and a basic collider parameter optimization [7].

In Ref. [8], the physics potentials of μp colliders with several energy and luminosity options (from $\sqrt{s}=314$ GeV, $L_{\mu p}=0.1$ fb^{-1} per year to $\sqrt{s}=4899$ GeV, $L_{\mu p}=280$ fb^{-1} per year) were studied. The sensitivity reach of each collider was calculated for some BSM phenomena such as R-parity violating squarks, leptoquarks, leptogluons and extra dimensions. Similarly, R-parity violating resonances were examined for a Tevatron based μp collider with $\sqrt{s}=0.9$ TeV and $L_{\mu p}=10^{32}cm^{-2}s^{-1}$ in Ref. [9]. In a recent study, excited muon production was analyzed at muon-hadron colliders based on the FCC [10].

This paper presents a follow-up to our previous study, which was based on the search potential of the FCC-based ep colliders for color octet electrons [11] (there are a number of other papers devoted to the study of color octet electron production at the LHC [12–15] and LHeC [16–18]).

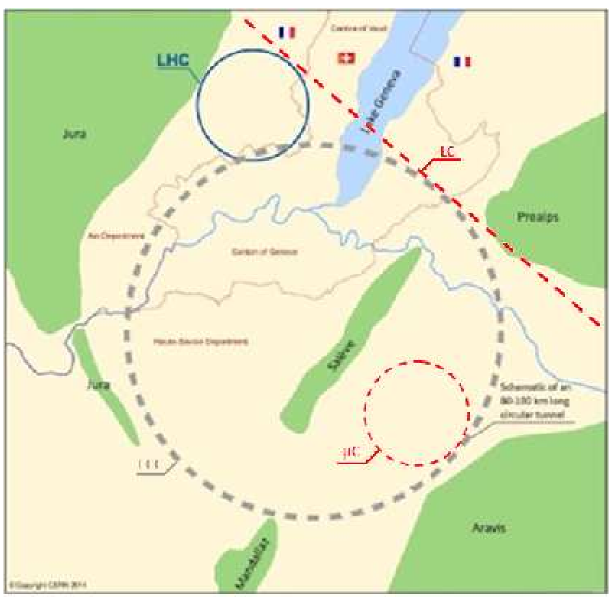

Fig. 1. (color online) Possible configuration of the FCC, linear collider (LC) and muon collider (μC).

We now consider another design, namely, the construction of a muon ring tangential to the FCC, which is schematically shown in Fig. 1. The aim is to achieve the highest possible CM energies in lepton-hadron colliders in order to make some of BSM physics research possible. Here, the physics potential of these future colliders is revealed by quantitatively exploring resonant production of color octet muons. Parameters of the potential FCC-based muon proton colliders are given in Table 1. The first four colliders [7] use the most recent design parameters from the MAP [1]. The last row corresponds to the ultimate case with 20 TeV muon beams in the FCC tunnel. The 20 TeV choice is due to the synchrotron radiation loss of muons, which is desired to be limited to 1 GeV/turn for a muon accelerator with 100 km circumference [19].

Table 1. Main parameters of potential FCC-based μp colliders.

collider name	E_μ /TeV	CM energy /TeV	$L_{\rm int}$/fb^{-1} /(per year)
μ63⊗FCC	0.063	3.55	0.02
μ750⊗FCC	0.75	12.2	5
μ1500⊗FCC	1.5	17.3	5
μ3000⊗FCC	3.0	24.5	5
μ20000⊗FCC	20	63.2	10

The rest of the paper is organized as follows. In Section 2, we present the phenomenology of color octet muons. Section 3 covers signal-background analyses and is closed by giving the results of discovery limit searches for muon-proton colliders. Section 4 addresses the determination of compositeness scales via muon-proton collider options under two possible cases regarding the results of the FCC. Finally, Section 5 contains a summary of the obtained results.

2 Color octet muons

One possible answer to the problems mentioned in the Introduction may hide behind the concept of compositeness. Fermion-scalar and three-fermion models are the most proper options which enable the known SM leptons to be constructed from more fundamental particles, namely preons. If the SM leptons are composed of color triplet fermions and color triplet scalars, then both fermion-scalar and three-fermion models predict at least one color octet partner to the color singlet leptons:

$$\ell=(F\bar{S})=3\otimes\bar{3}=1\oplus 8, \tag{1}$$

$$\ell=(FFF)=3\otimes 3\otimes 3=1\oplus 8\oplus 8\oplus 10. \tag{2}$$

The interaction Lagrangian of ℓ_8 with leptons and gluons can be written as

$$L=\frac{1}{2\Lambda}\sum_{l}\left\{\bar{\ell_8^\alpha}g_{\rm s}G^\alpha_{\mu\nu}\sigma^{\mu\nu}(\eta_{\rm L}\ell_{\rm L}+\eta_{\rm R}\ell_{\rm R})+{\rm h.c.}\right\} \tag{3}$$

where $g_{\rm s}$ is the strong coupling constant, Λ denotes the compositeness scale, $G_{\mu\nu}$ is the gluon field strength tensor, $\ell_{\rm L(R)}$ stands for left (right) spinor components of lepton, $\ell=e,\mu,\tau$; $\sigma^{\mu\nu}$ is the antisymmetric tensor ($\sigma^{\mu\nu}=\frac{i}{2}[\gamma^\mu,\gamma^\nu]$), and $\eta_{\rm L}(\eta_{\rm R})$ symbolizes chirality factor. Keeping in mind leptonic chiral invariance ($\eta_{\rm L}\eta_{\rm R}=0$), we

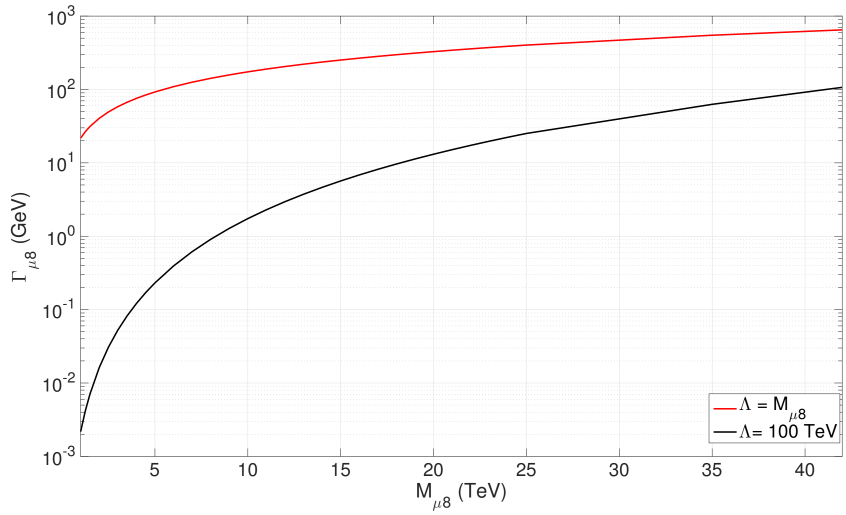

Fig. 2. (color online) color octet muon decay width for $\Lambda = M_{\mu 8}$ and Λ=100 TeV.

take $\eta_L = 1$ and $\eta_R = 0$. The decay width of ℓ_8 is given by

$$\Gamma(\ell_8 \rightarrow \ell + g) = \frac{\alpha_s M_{\ell_8}^3}{4\Lambda^2}, \tag{4}$$

where $\alpha_s = g_s/4\pi$. The dependence of the decay width on the mass of μ_8 is presented in Fig. 2 for the $\Lambda = M_{\mu_8}$ and Λ=100 TeV cases.

The resonant μ_8 production (see Fig. 3) cross sections for different stages of the FCC-based μp colliders from Table 1 were calculated using the MadGraph5 event generator [20]. The CTEQ6L1 parametrization [21] was used as the parton distribution function and the results are presented in Fig. 4. The MadGraph5-Pythia6 interface was used for parton showering and hadronization [22]. The same tools were used for the rest of the study and further calculations did not take detector effects into account.

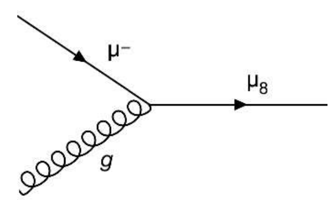

Fig. 3. Feynman diagram for resonant μ_8 production.

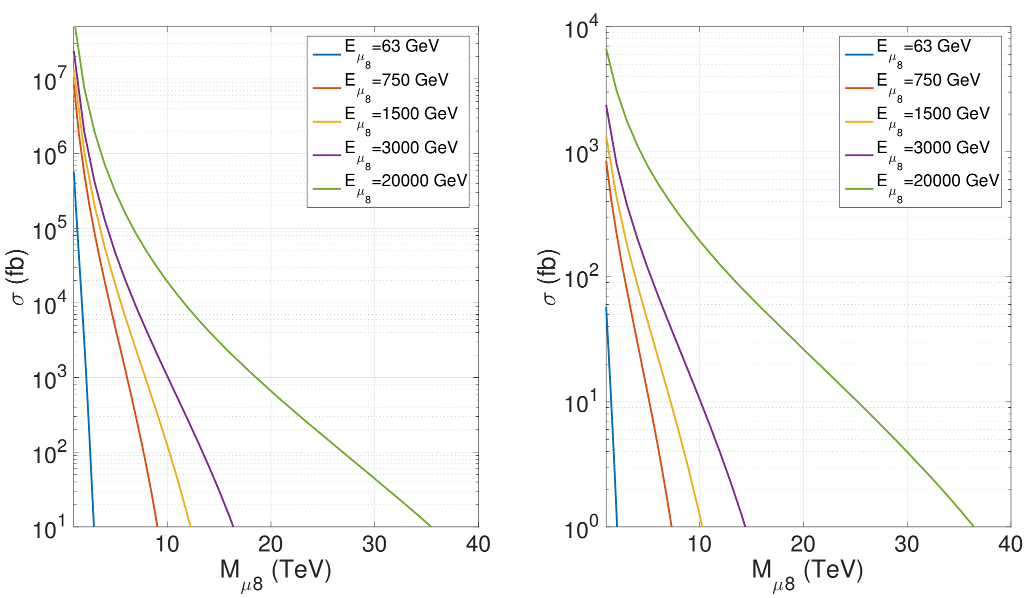

Fig. 4. (color online) Resonant color octet muon production at the FCC-based μp colliders given in Table 1 for (a) $\Lambda = M_{\mu 8}$ and (b) Λ=100 TeV ($\mu p \rightarrow \mu_8 X \rightarrow \mu j X$).

3 Signal - background analysis

In this section, results of the numerical calculations are shown for the process pμ → jμ to leading order in order to analyze the search potential of the FCC-based muon-proton colliders for μ_8 discovery via resonant production within the $\Lambda = M_{\mu 8}$ scenario. Jets correspond to gluons for signal ($\mu g \to \mu_8 \to \mu g$ at partonic level) and quarks for main background (μq→μq through γ and Z exchanges) processes.

A staged approach was applied to determine the mass limits, as follows. μ63⊗FCC, the μp collider with minimum CM energy, was chosen as the initial collider where the discovery limit of the μ_8 mass was to be sought. After the discovery limit was determined, a worse scenario was considered where μ_8 was assumed to have a larger mass. It was supposed that the previous collider had excluded the μ_8 mass up to the corresponding discovery limit and necessary cuts regarding this assumption were applied for the next higher CM energy μp collider. Latter colliders, following the rows of Table 1, were treated in the same way. This procedure ends up with the ultimate μp collider with CM energy 63.2 TeV which was given in the last row of Table 1. One should note that a sequential building of these colliders is not realistic. Therefore, if a muon-proton collider is built, color-octet muon search discovery cuts would depend on up-to-date experimental exclusion limits.

Kinematical distributions of μ63⊗FCC with generic cuts ($p_{\mathrm{T}_\mu} > 20$ GeV, $p_{\mathrm{T}_j} > 30$ GeV) are given in Fig. 5. Reconsideration of the ATLAS/CMS results in the search for second generation leptoquarks [23, 24] (which have the same decay channel as μ_8) leads us to the strongest current limit on the color octet muon mass, $M_{\mu_8} \gtrsim 1$ TeV. Therefore, we chose the discovery cut for transverse momentum to be $p_{\mathrm{T}} > 350$ GeV on our initial μp collider. This transverse momentum cut was applied on the final state muon as well as the leading jet. In order to suppress the background while keeping the signal cross section as much as possible, the following pseudorapidity cuts were also applied: $2.00 < \eta_j < 4.00$, $0.5 < \eta_\mu < 4.74$. The maximum possible value of η_μ and η_j was taken as 4.74, which corresponds to 1^o in the proton direction. This value can be covered by a very forward detector as in the LHeC case [25]. The effects of these discovery cuts can be seen by comparing Fig. 5(d) with Fig. 6, where the invariant mass of μ_8 was reconstructed from final state particles μ and the leading jet. After these cuts, the signal cross sections signals remained almost the same while the background cross-section decreased significantly.

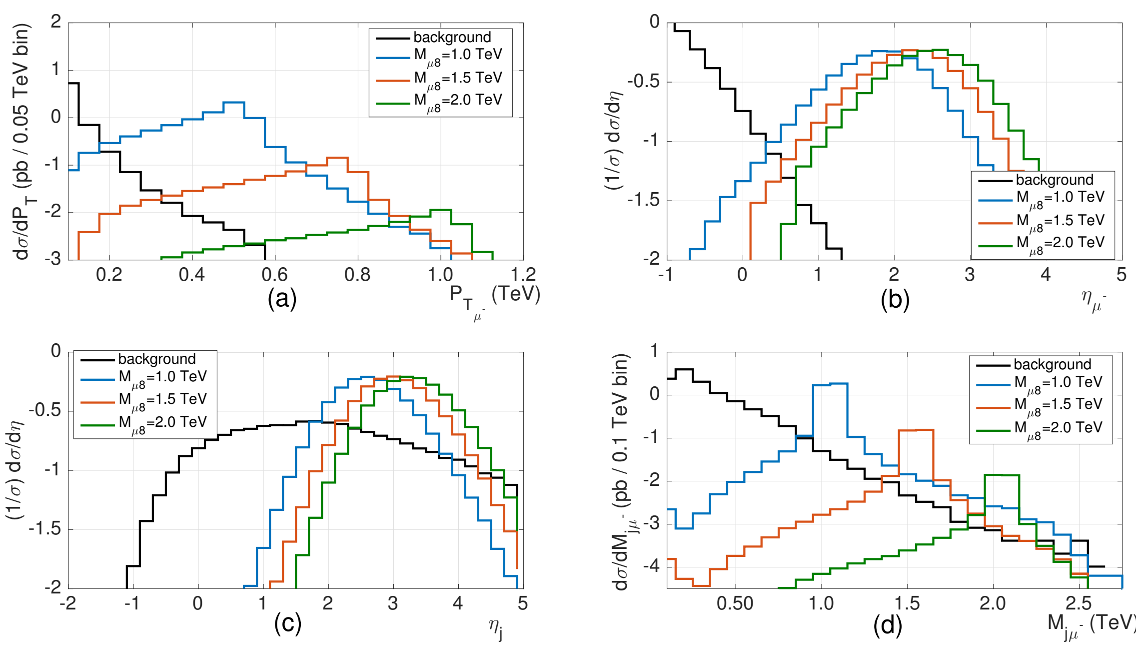

Fig. 5. (color online) (a) Transverse momentum distributions of final state muons (almost the same distribution holds for the leading jets); (b) pseudorapidity distributions of final state muons; (c) pseudorapidity distributions of final state jets; and (d) invariant mass distributions for signal and background at μ63⊗FCC after generic cuts.

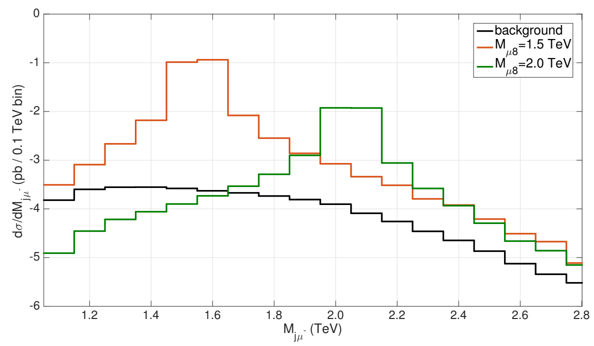

Fig. 6. (color online) Invariant mass distributions for signal and background at $\mu63\otimes$FCC after discovery cuts.

Statistical significance (SS) is calculated using the formula below:

$$SS=\sqrt{2L_{\rm int}}\sqrt{(\sigma_{\rm S}+\sigma_{\rm B})\ln(1+(\sigma_{\rm S}/\sigma_{\rm B}))-\sigma_{\rm S}}, \qquad (5)$$

where $\sigma_{\rm S}$ and $\sigma_{\rm B}$ denote the cross-section values of signal and background, respectively. The integrated luminosity values, $L_{\rm int}$, of each collider per year was estimated in Ref. [7]. Discovery (SS=5) and observation (SS=3) limits for 0.02 fb^{-1} $\mu63\otimes$FCC integrated luminosity were found to be 2380 and 2460 GeV, respectively. Regarding these results for the minimum energy μp collider, $p_{\rm T}>800$ GeV was considered appropriate for the next stage $\mu750\otimes$FCC and similar analyses were performed. These consecutive calculations gave us the mass reach of each collider as given in Table 2. The applied discovery cuts are also given in the same table. The mass window formulation was kept the same for all calculations: $M_{\mu8}-2\Gamma_{\mu8}<M_{\mu8}<M_{\mu8}+2\Gamma_{\mu8}$. Signal and background event numbers were calculated directly in this mass window without using any binning algorithm. The invariant mass distributions after discovery cuts for the higher energy colliders are presented in Fig. 7.

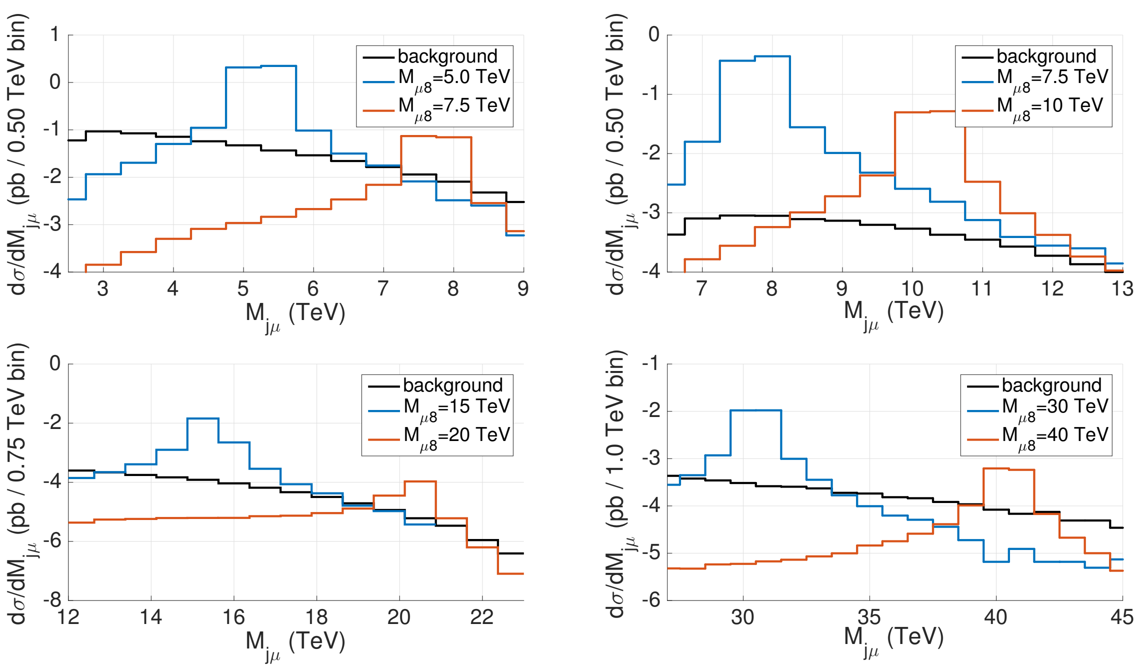

Fig. 7. (color online) Invariant mass distributions for signal and background after discovery cuts at (a) $\mu750\otimes$FCC, (b) $\mu1500\otimes$FCC, (c) $\mu3000\otimes$FCC and (d) the ultimate case $\mu20000\otimes$FCC colliders.

4 Limits on compositeness scale

If the μ_8 is discovered by the FCC-pp option, μp colliders will give an opportunity to estimate the compositeness scale. In this regard, two distinct possibilities should be considered:

a) μ_8 is discovered by the FCC but not observed at μ-FCC. In this case one can put a lower limit on compositeness scale,

b) μ_8 is discovered by the FCC and also observed at μ-FCC. In this case one can determine the compositeness scale.

Table 2. Kinematical discovery cuts and observation (3σ) and discovery (5σ) limits for μ_8 at different μp colliders. Transverse momentum cuts are given in TeV. Significance values are calculated locally.

collider name	$L_{\rm int}/{\rm fb}^{-1}$	Kinematical cuts					$M_{\mu 8}$ ±PDF% ±scale%/TeV			
		$p_{\rm T_{min}}$	$\eta_{\mu_{\rm min}}$	$\eta_{\mu_{\rm max}}$	$\eta_{j_{\rm min}}$	$\eta_{j_{\rm max}}$	3σ		5σ	
μ63⊗FCC	0.02	0.350	0.5	4.74	2.0	4.0	2.46	+2.60% +1.63% -1.83% -1.75%	2.38	+2.52% +1.68% -2.10% -1.89%
μ750⊗FCC	5	0.800	-1.3	4.74	1.0	4.1	9.60	+1.34% +0.63% -1.15% -1.27%	9.21	+1.46% +0.74% -1.20% -1.37%
μ1500⊗FCC	5	3.00	-1.7	4.74	0.7	3.9	13.8	+1.30% +0.51% -1.01% -0.87%	13.2	+ 1.36% +0.53% -1.14% -1.06%
μ3000⊗FCC	5	4.40	-2.1	4.74	0.3	3.5	18.9	+1.22% +0.53% +1.27% +0.44%	18.1	-1.01% -0.63% -1.22% -0.77%
μ20000⊗FCC	10	6.00	-2.7	4.74	-0.7	2.7	42.7	+1.57% +0.59% -1.29% -0.58%	41.5	+1.61% +0.63% -1.40% -0.60%

In this section we present analyses of these two possibilities for four different benchmark points, namely, M_{μ_8}=2.5,5,7.5 and 10 TeV.

4.1 μ_8 discovered by FCC but not observed at μ-FCC

If we assume that the μ_8 mass is found from FCC results, then it is possible to determine optimal cuts for given M_{μ_8} at the μ-FCC colliders. Let us start by considering M_{μ_8}=5.0 TeV at μ750⊗FCC.

It is seen from Fig. 8 that $-1.3<\eta_\mu<4.74$ and $0.7<\eta_j<3.3$ cuts drastically decrease the background, whereas the signal is only slightly affected. Similar cuts were determined for other μ-FCC collider options and M_{μ_8} values, and these optimal cuts are presented in Table 3. The invariant mass window $0.99M_{\mu_8}<M_{\mu j}<1.01M_{\mu_8}$ has been used in this particular analysis. The μ63⊗FCC collider was not included in this section due to its remarkably low potential compared to the other options.

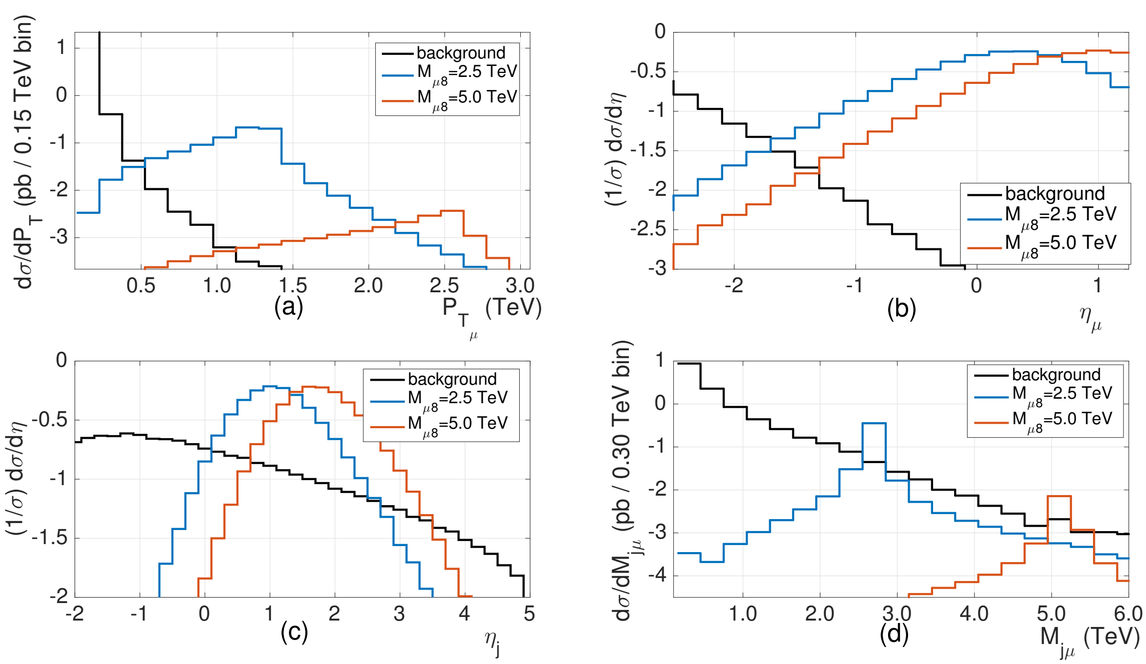

Fig. 8. (color online) (a) Transverse momentum distributions of final state muons (almost the same distribution holds for the leading jets); (b) pseudorapidity distributions of final state muons; (c) pseudorapidity distributions of final state jets; and (d) invariant mass distributions for signal and background at μ750⊗FCC after generic cuts.

Table 3. Optimal cuts for determination of compositeness scale lower bounds.

collider	cut type	M_{μ_8}=2.5 TeV		M_{μ_8}=5.0 TeV		M_{μ_8}=7.5 TeV		M_{μ_8}=10 TeV	
		min	max	min	max	min	max	min	max
μ750⊗FCC	η_μ	-1.7	4.74	-1.3	4.74	-1.2	4.74	-	-
	η_j	0.2	2.6	0.7	3.3	1.0	3.9	-	-
	mass window/GeV	2475	2525	4950	5050	7425	7575	-	-
μ1500⊗FCC	η_μ	-2.3	4.74	-2.0	4.74	-1.8	4.74	-1.7	4.74
	η_j	-0.6	1.9	-0.1	2.7	0.4	3.1	0.5	3.5
	mass window/GeV	2475	2525	4950	5050	7425	7575	9900	10100
μ3000⊗FCC	η_μ	-2.9	4.74	-2.7	4.74	-2.5	4.74	-2.3	4.74
	η_j	-1.4	1.4	-0.8	2.1	-0.4	2.6	-0.2	3.1
	mass window/GeV	2475	2525	4950	5050	7425	7575	9900	10100
μ20000⊗FCC	η_μ	-3.9	4.74	-3.5	4.74	-3.3	4.74	-3.2	4.74
	η_j	-3.0	-0.9	-2.5	0.1	-2.1	0.5	-1.9	1.0
	mass window/GeV	2475	2525	4950	5050	7425	7575	9900	10100

Table 4. Lower limits on compositeness scale, in TeV, at the FCC-based μp colliders.

collider	$L_{\rm int}/{\rm fb}^{-1}$	M_{μ_8}=2.5 TeV		M_{μ_8}=5.0 TeV		M_{μ_8}=7.5 TeV		M_{μ_8}=10 TeV	
		3σ	5σ	3σ	5σ	3σ	5σ	3σ	5σ
μ750⊗FCC	5	270	210	170	130	50	35	-	-
μ1500⊗FCC	5	360	280	220	170	130	100	55	40
μ3000⊗FCC	5	475	370	320	245	230	170	140	105
μ20000⊗FCC	10	1390	1080	850	655	515	400	315	246

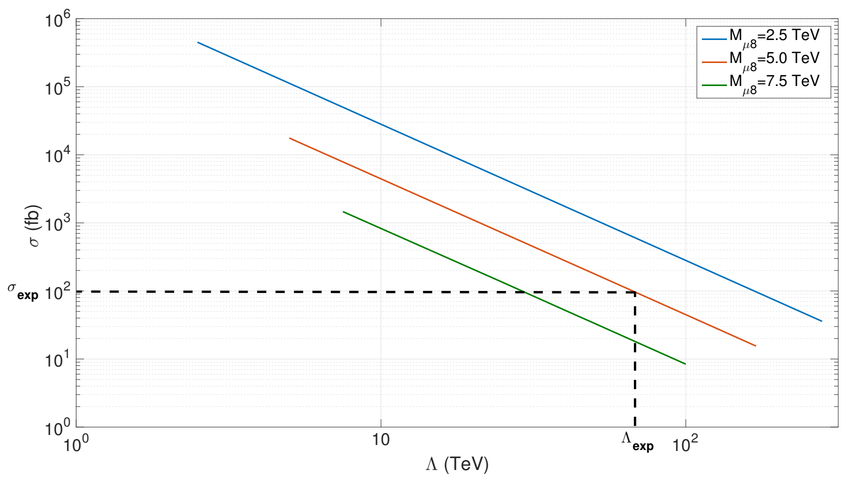

Fig. 9. (color online) Cross section distributions with respect to compositeness scale for the μ1500⊗FCC collider.

Applying the cuts presented in Table 3 and $p_{\rm T}>350$ GeV for all cases, one can estimate achievable lower limits on compositeness scale. Using Eq. (5), we obtain the Λ values given in Table 4. As expected, lower bounds on compositeness scale are decreased with increasing value of the μ_8 mass. It is seen that multi-hundred TeV lower bounds can be put on the compositeness scale if μ_8 is discovered at the FCC and not observed at any $\mu\otimes$ FCC.

4.2 μ_8 discovered by FCC and observed at μ-FCC

In this case, the value of cross section at the μp colliders, which is inversely proportional to Λ^2, gives the opportunity to determine the compositeness scale directly. As an example, let us consider the μ1500⊗FCC case. In Fig. 9 we present the Λ dependence of μ_8 production cross section for $M_{\mu_8}=2.5, 5, 7.5$ TeV. Supposing that the FCC discovers μ_8 with 5 TeV mass, and μ1500-FCC measures the cross section as $\sigma_{\rm exp}\sim 100$ fb, one can derive the compositeness scale as $\Lambda_{\rm exp}\simeq 70$ TeV.

4.3 μ_8 not discovered by FCC but observed at μ-FCC

Another possibility is the failure of the μ_8 search at the FCC. This can be caused by the value of color-octet muon mass, $M_{\mu 8}$, which can be greater than the discovery limit of the FCC itself. In this case, the advantages of μ-FCC colliders with quite large discovery limits manifest themselves.

5 Conclusion

Discovery mass limits for μ_8 at muon, proton and FCC-based μp colliders are shown in Fig. 10. It is obvious that discovery mass limits for pair production of μ_8 at muon colliders are approximately half the CM energies. Discovery limit values for the LHC and FCC are obtained by rescaling ATLAS/CMS second generation LQ results [23, 24] using the method developed by G. Salam and A. Weiler [26]. Following Ref. [27], integrated luminosity values of 3 ab^{-1} and 20 ab^{-1} have been used for the High Luminosity LHC (HL-LHC) and the FCC-hh, respectively. As can be seen from Fig. 10, FCC based μp colliders with a discovery limit up to 40 TeV are the most advantageous of the other collider options for μ_8 searches. Moreover, FCC-based μp colliders would give the opportunity to probe compositeness up to the PeV scale.

The authors are grateful to Saleh Sultansoy for useful discussions. The authors are also grateful to Subhadip Mitra and Tanumoy Mandal for sharing their leptogluon MadGraph model file.

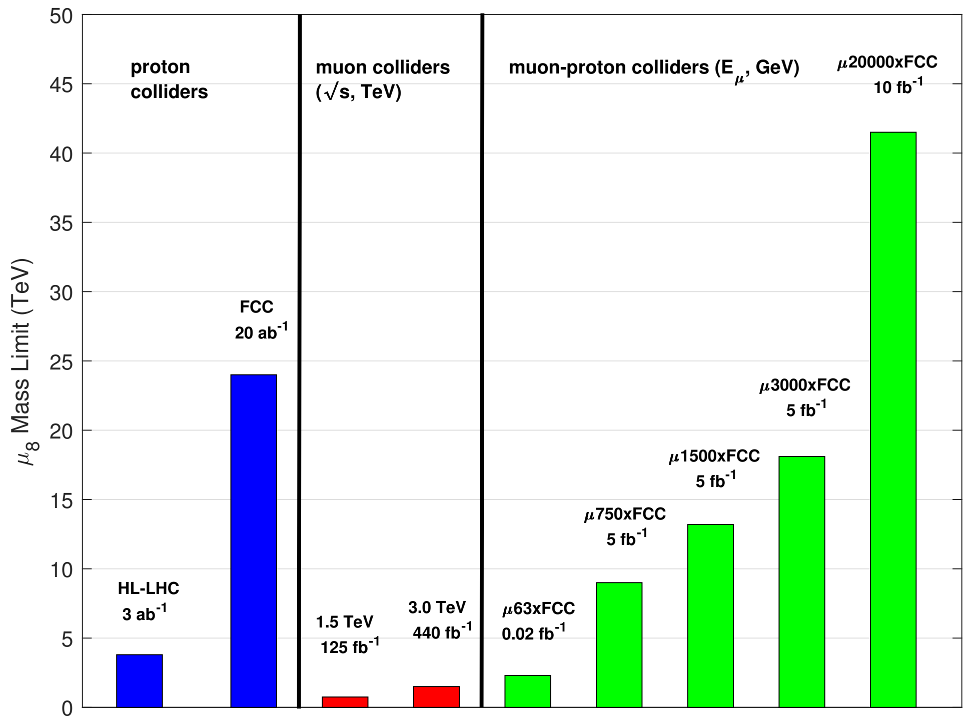

Fig. 10. (color online) Mass discovery limits ($SS=5$) of the color octet muon for different types of collider, i.e. proton, muon and muon-proton.

References

1 J. P. Delahaye et al, *Enabling intensity and energy frontier science with a muon accelerator facility in the U.S.*, arXiv:1308.0494v2 [physics.acc-ph]

2 B.J. King, *Parameter Sets for 10 TeV and 100 TeV Muon Colliders, and their Study at the HEMC'99 Workshop*, arXiv:physics/0005008 [physics.acc-ph]

3 FCC web page: https://fcc.web.cern.ch.

4 I.F. Ginzburg, Physics at future e p, gamma p (linac-ring) and mu p colliders, Turk J. Phys., **22**: 607 (1998)

5 S. Sultansoy, *The post-HERA era: brief review of future lepton-hadron and photon-hadron colliders*, DESY 99-159, arXiv:hep-ph/9911417v2

6 V. D. Shiltsev, *An asymmetric muon proton collider: luminosity consideration*, in Proceedings of 1997 Particle Accelerator Conference, 1998 (Vancouver, British Columbia, Canada), p. 420

7 Y.C. Acar et al, *FCC Based Lepton-Hadron and Photon-Hadron Colliders: Luminosity and Physics*, arXiv:1608.02190 [physics.acc-ph]

8 K. Cheung, *Muon-proton colliders: Leptoquarks, contact interactions and extra dimensions*, AIP Conference Proceedings, **542**: 160 (2000)

9 M. Carena, D. Choudhury, C. Quigg, and S. Raychaudhuri, Phys. Rev. D, **62**(9): 095010 (2000)

10 A. Caliskan, S. O. Kara, and A. Ozansoy, *Excited muon searches at the FCC based muon-hadron colliders*, arXiv:1701.03426 [hep-ph]

11 Y. C. Acar, U. Kaya, B. B. Oner, and S. Sultansoy, *Color octet electron search potential of the FCC based e-p colliders*, arXiv:1605.08028v2 [hep-ph]

12 A. Celikel, M. Kantar, and S. Sultansoy, Phys. Lett. B, **443**(1): (1998)

13 T. Mandal and S. Mitra, Phys. Rev. D, **87**(9): (2013) arXiv:1211.6394v2 [hep-ph]

14 D. Gonalves-Netto, D. Lpez-Val, K. Mawatari, I. Wigmore , and T. Plehn, Phys. Rev. D, **87**(9): (2013), arXiv:1303.0845v1 [hep-ph]

15 T. Mandal, S. Mitra, and S. Seth, Phys. Lett. B, **758**: (2016), arXiv:1602.01273v2 [hep-ph]

16 A. Celikel and M. Kantar, Tr. J. of Physics, **22**: 401 (1998)

17 M. Sahin, S. Sultansoy, and S. Turkoz, Phys. Lett. B, **689**: 172 (2010)

18 M. Sahin, Acta Physica Polonica B, **45**: 1811 (2014)

19 S. Sultansoy talk at 1^{st} FCC Physics Workshop (CERN), https://indico.cern.ch/event/550509/contributions/2413830

20 J. Alwall et al, JHEP, 2014(7) (2014); arXiv:1405.0301v2 [hep-ph]

21 D. Stump et al, JHEP, **0310**: 046 (2003)

22 T. Sjostrand, S. Mrenna, and P.Z. Skands, JHEP, **0605**: 026 (2006) arXiv:hepph/0603175 [hep-ph]

23 V. Khachatryan et al (CMS Collaboration), Phys. Rev. D, **93**: 032004 (2016)

24 ATLAS Collaboration, *Search for scalar leptoquarks in pp collisions at* $\sqrt{s}$*=13 TeV with the ATLAS experiment*, arXiv:1605.06035v2 [hep-ex]

25 J. L. Abelleira Fernandez et al (LHeC Study Group), J. Phys. G: Nucl. Part. Phys., **39**: 075001 (2012)

26 G. Salam and A. Weiler, *The Collider Reach project*, http://collider-reach.web.cern.ch/collider-reach

27 M. Benedikt, X. Buffat, D. Schulte, and F. Zimmermann, *Luminosity targets for FCC-hh*, in Proceedings of 2016 International Particle Accelerator Conference (Busan, Korea), p.1523